Supporting Information

for ***Physical Chemistry Chemical Physics***

Supporting Information

Construction of High Efficiency Non-doped Deep Blue Eimitter Based on Phenanthroimidazole: Remarkable Substitution Effects on the Excited State Properties and Device Performance

Zhiming Wang[a], Ying Feng[a], Shitong Zhang[b] , Yu Gao[b], Zhao Gao[b], Yanming Chen[a], Xiaojuan Zhang[a], Ping Lu[b], Bing Yang[b], Ping Chen[c]*, Yuguang Ma[b], Shiyong Liu[c]*

[a] School of Petrochemical Engineering, Shenyang University of Technology, Liaoyang 111003, China

[b] State Key Laboratory of Supramolecular Structure and Materials, Jilin University, Changchun 130012, China

[c] State Key Laboratory on Integrated Optoelectronics, College of Electronic Science and Engineering, Jilin University, Changchun 130012, China

Contents

1. Synthesis

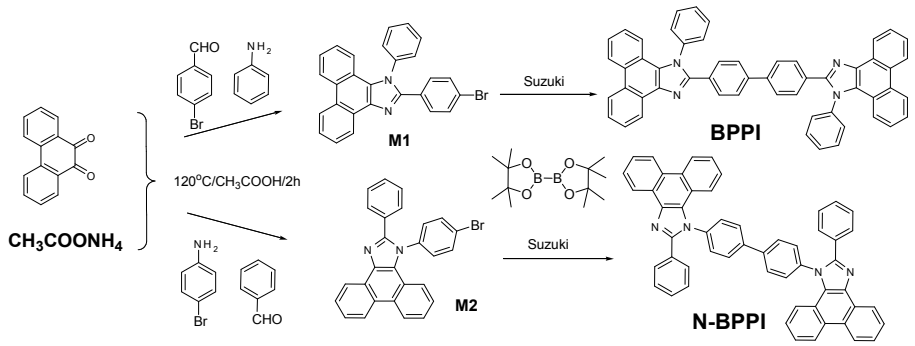

Scheme S1 The synthetic routes to **BPPI** and **N-BPPI.**

2-(4-bromophenyl)-1-phenyl-1H-phenanthro[9,10-d]imidazole (M1)

A mixture of aniline (4.7 g, 50.0 mmol), phenanthrenequinone (2.08 g, 10.0 mmol), benzaldehyde (1.85g, 10.0 mmol), ammonium acetate (3.08 g, 40.0mmol), and acetic acid (80 mL) was heated under nitrogen in an oil bath to 120 °C. The mixture was maintained at this temperature for 2 h, and then cooled and filtered. The solid product was washed with an acetic acid/water mixture (1:1, 150 mL X 2), and washed with water to obtain the light-yellow crystals (4.09 g, 91.4% yield). ^{1}H NMR (500 MHz, DMSO, ppm): 8.94 (d, 1H), 8.88 (d, 1H), 8.69 (d, 1H), 7.78 (t, 1H), 7.75-7.60 (m, 6H), 7.60-7.54 (m, 3H), 7.50 (d, 2H), 7.34 (t, 1H), 7.08 (d, 1H). MALDI-TOF (*m*/*z*): [M+] calcd. $C27H_{17}N_2Br$, 448.06; found, 450.3.

1-(4-bromophenyl)-2-phenyl-1H-phenanthro[9,10-d]imidazole (M2)

A mixture of 4-bromobenzenamine (8.5 g, 50.0 mmol), phenanthrenequinone (2.08 g, 10.0 mmol), benzaldehyde (1.06g, 10.0 mmol), ammonium acetate (3.08 g, 40.0mmol), and acetic acid (80 mL) was heated under nitrogen in an oil bath to a bath temperature of 120 °C, The mixture was maintained at this temperature for 2 h, and then cooled and filtered. The solid product was washed with an acetic acid/water mixture (1:1, 150 mL X 2) and washed with water to obtain the light-yellow crystals (4.19 g, 93.0% yield). ^{1}H NMR (500 MHz, DMSO, ppm): 8.95 (d, 1H), 8.89 (d, 1H), 8.73 (d, 1H), 7.89(d, 1H), 7.78 (t, 1H), 7.73-7.64 (m, 4H), 7.47-7.31 (m, 3H), 7.10 (d,

1H). MALDI-TOF (*m*/*z*): [M+] calcd. $C_{27}H_{17}N_2Br$, 448.06; found, 451.3.

BPPI or N-BPPI: A mixture of M1 or M2 (0.5 g, 1.12 mmol), 4,4,4',4',5,5,5',5'-octamethyl-2,2'-bi(1,3,2- dioxaborolane) (0.15 g, 0.56 mmol), $Pd(PPh_3)_4$ (25 mg, 0.03 mmol), and sodium carbonate (0.53 g, 5 mmol) in THF (20 mL) and distilled water (2.5 mL) was refluxed for 2 d under nitrogen. The crude product was concentrated by rotary evaporation and filtered. After drying at 40°C in a vacuum baking oven, the powder was purified by column chromatography.

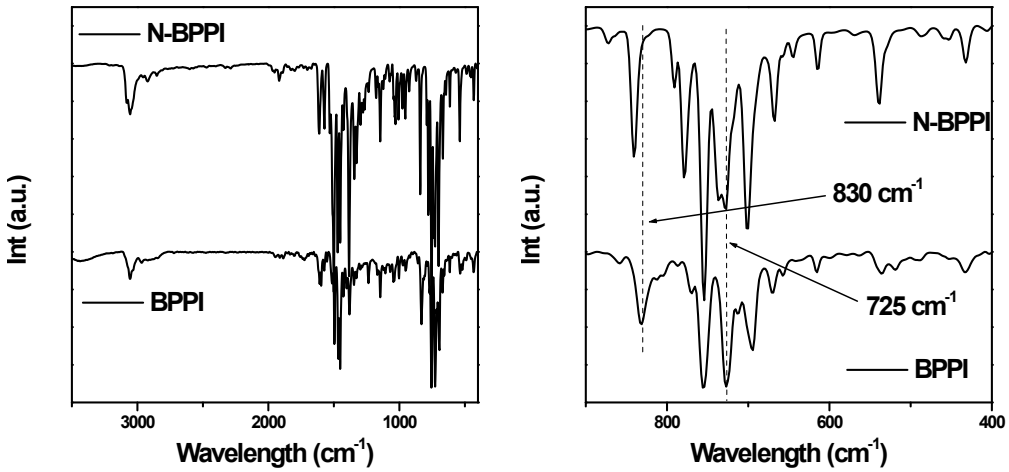

Fig. S1 FTIR spectra of **BPPI** and **N-BPPI.**

2. Thermal Properties

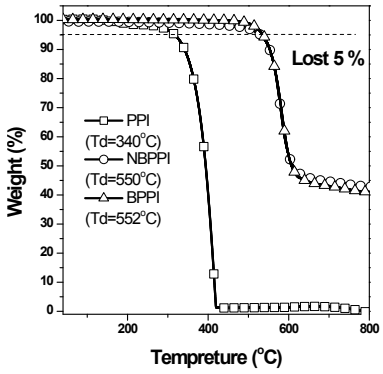

Fig. S2 The TGA graphs of **BPPI** and **N-BPPI**.

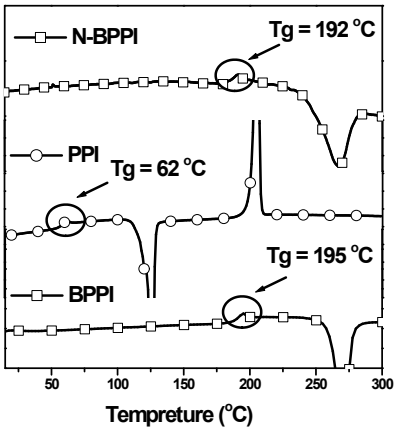

Fig. S3 The DSC graphs of PPI, **BPPI** and **N-BPPI**.

3. CV Measurements

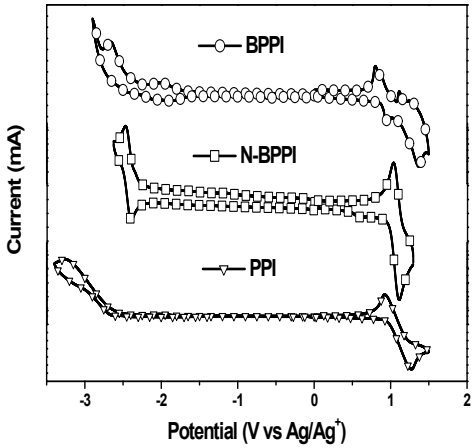

Fig. S4 The CV curve of PPI, **BPPI** and **N-BPPI**.

Tab. S1 Electrochemical data for PPI, **BPPI** and **N-BPPI**.

	E^{ox}_{onset} (V)	E^{red}_{onset} (V)	HOMO[a] (eV)	LUMO[a] (eV)	E_{gap} (eV)
PPI	0.95	-2.65	-5.53	-2.07	3.46
BPPI	0.89	-2.43	-5.47	-2.29	3.18
NBPPI	0.98	-2.34	-5.59	-2.34	3.32

[a]. Calculated by comparing with ferrocene (Fc) (4.8 eV) and calibrated using $E_{1/2}$ (Fc/Fc^+) measurement.

Because the electrolyte concentration influenced the onset oxidation/reduction potential, the values of HOMO/LUMO was inaccurate by estimating only from the data above. For increasing the accuracy, the ferrocene was usually applied as a reference to calibrate this difference. Concretely in every measurement, the compound

was dissolved in CH_2Cl_2 or DMF with ~0.1 M tetra-n-butylammonium - hexafluorophosphate (n-Bu_4NPF_6) at room temperature, and the CV sweep was done to get the onset oxidation/reduction potential (E^{ox}_{onset} or E^{red}_{onset}). In the same concentration of electrolyte, the CV sweep of ferrocene was also done to gain the calibrated value of $E_{1/2}$ (Fc/Fc^+). At last, the more accurate values of HOMO/LUMO were calculated as below:

$$E_{HOMO} = -|eE^{ox}_{onset} + (4.80eV - E_{1/2}(Fc/Fc^+))|$$

$$E_{LUMO} = -|eE^{red}_{onset} + (4.80eV - E_{1/2}(Fc/Fc^+))|$$

4. Optimized structures of BPPI and N-BPPI

Table.S2 The optimized twist angles in the lowest energy ground state.

	N1-TA	*C2*-TA	B-TA
BPPI	**80.6 °**	**30.2 °**	**33.6 °**
N-BPPI	**77.7 °**	**32.3 °**	**37.1 °**

5. S1 to S10 NTO of BPPI and N-BPPI

BPPI

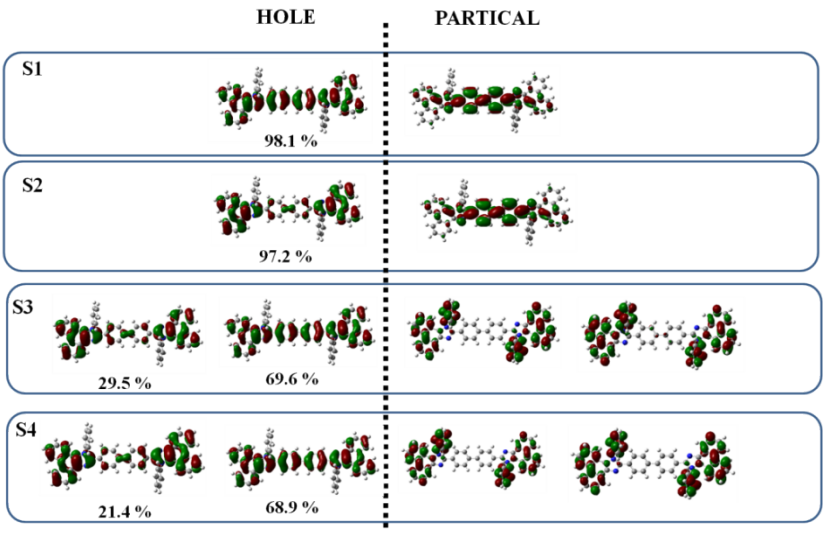

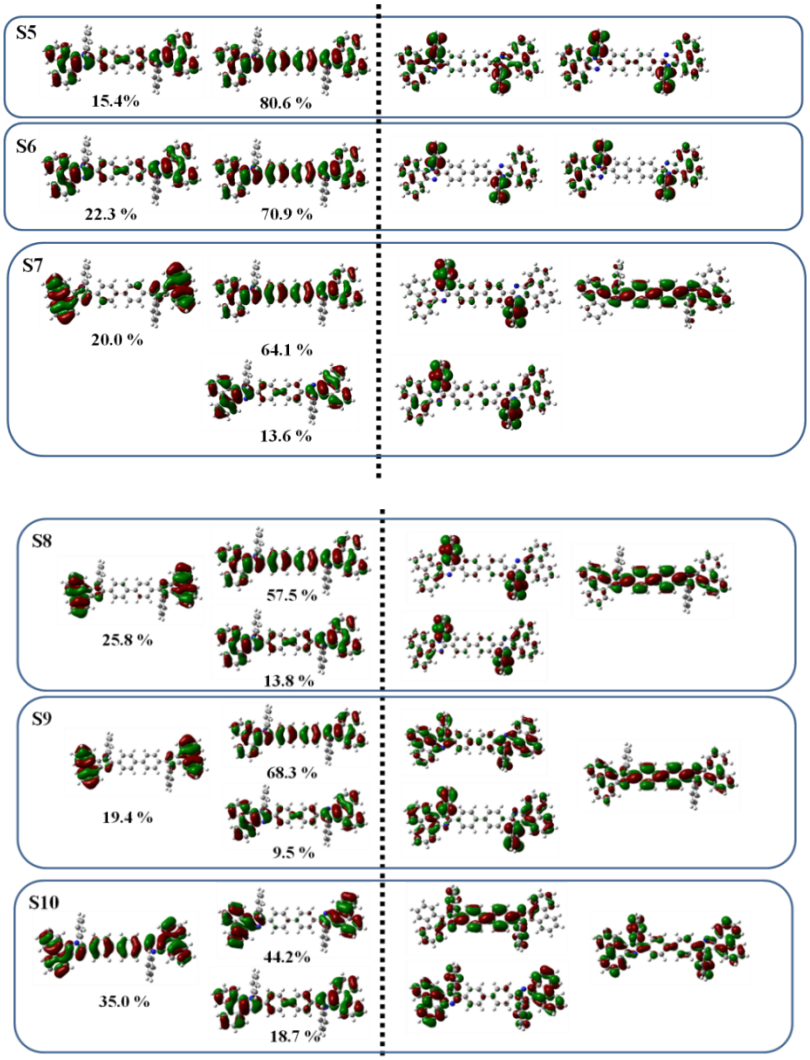

Fig. S5 S1 to S10 NTO of BPPI

N-BPPI

Fig. S6 S1 to S10 NTO of N-BPPI

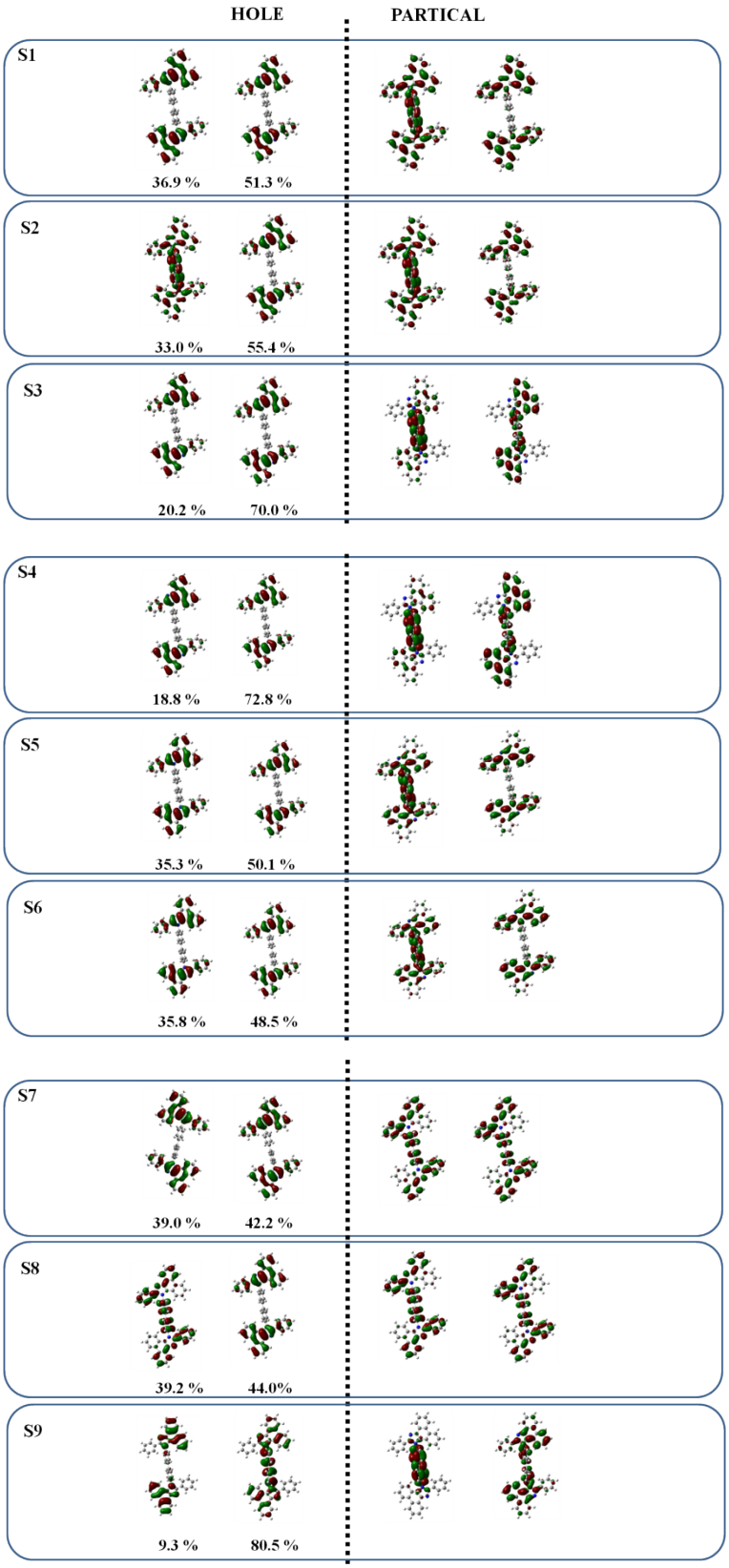
HOLE
PARTICAL
S1
36.9 %
51.3 %
S2
33.0 %
55.4 %
S3
20.2 %
70.0 %
S4
18.8 %
72.8 %
S5
35.3 %
50.1 %
S6
35.8 %
48.5 %
S7
39.0 %
42.2 %
S8
39.2 %
44.0%
S9
9.3 %
80.5 %

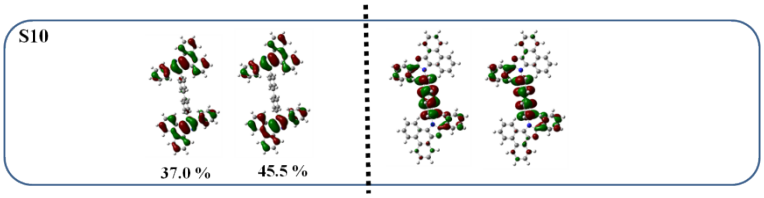

6. The solvatochromic Lippert-Mataga model

The Lippert-Mataga model is estimated according to **Equation 1** as shown below:

$$hc(\nu_a - \nu_f) = hc(\nu_a^0 - \nu_f^0) + \frac{2(\mu_e - \mu_g)2}{a_0^3} f(\varepsilon,n) \qquad \textbf{Equation 1}$$

where h is the Plank constant, c is the light speed in vacuum, $f(\varepsilon,n)$ is the orientational polarizability of solvents and $f(\varepsilon,n) = \left[\frac{\varepsilon - 1}{2\varepsilon + 1} - \frac{n^2 - 1}{2n^2 - 1}\right]$, $\nu_a^0 - \nu_f^0$ is the Stokes shifts when f is zero, a_0 is the solvent Onsager cavity radius, μ_e and μ_g are dipole moments of excited-state and ground-state, respectively. ε is the solvent dielectric constant and n is the solvent refractive index. a_0 and μ_g were estimated at the level of b3lyp/6-31g(d,p) from the Gaussian09 package.

Results: **BPPI**(a_0=0.714 nm and μ_g = 4.579D) **N-BPPI** (a_0=0.699 nm and μ_g = 0.2693D)

Table-S3 The solvatochromic properties of BPPI

BPPI				
Solvents	$f(\varepsilon,n)$	λ_a (nm)	λ_f (nm)	$\nu_a - \nu_f$ (cm^{-1})
Hexane	0.0012	368	412	2902.06838
Ethylamine	0.048	369	414	2945.68163
Butylether	0.096	370	415	2930.64148
Ethylether	0.167	368	415	3077.52750
Ethylacetate	0.2	368	419	3307.56459
Tetrahydrofuran	0.21	369	421	3347.30188
Acetone	0.284	366	443	4749.04094
Acetonitrile	0.305	365	445	4925.35016

In low-polarity solvents (the former six):

Slope = 2093.37370337; Correlation = 0.90452685; μ_e = 7.80178524

In high-polarity solvents (the latter five):

Slope = 14721.10104476; Correlation = 0.98619292; μ_e = 20.68905984

Table-S4 The solvatochromic properties of N-BPPI

N-BPPI				
Solvents	$f(\varepsilon,n)$	λ_a (nm)	λ_f (nm)	ν_a - ν_f (cm^{-1})
Hexane	0.0012	360	363	229.56841
Ethylamine	0.048	361	365	303.57075
Butylether	0.096	361	366	378.42665
Ethylether	0.167	360	366	455.37341
Ethylacetate	0.2	361	369	600.56002
Tetrahydrofuran	0.21	360	369	677.50678
Acetone	0.284	359	373	1045.50173
Acetonitrile	0.305	357	374	1273.23657

In all solvents:

Slope = 3176.50335005; Correlation = 0.93557306; μ_e = 9.61048417

7. Electroluminescence devices

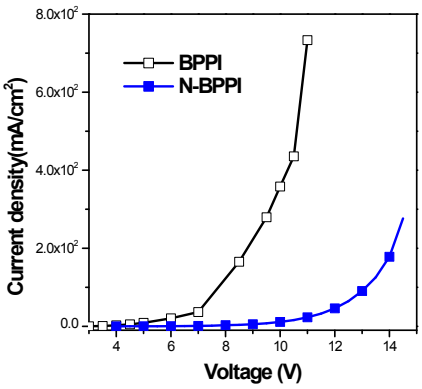

Fig. S7 The current density versus voltage in the **BPPI** and **N-BPPI** devices.

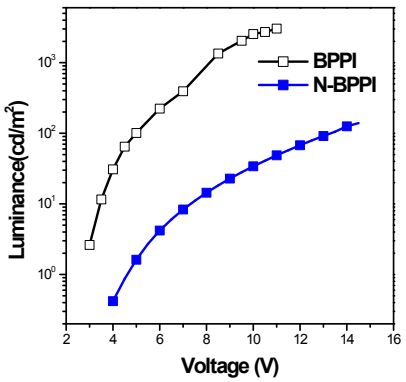

Fig. S8 The luminance versus voltage in the **BPPI** and **N-BPPI** devices.